

Collapse of Uniformly Rotating Stars to Black Holes and the Formation of Disks

Stuart L. Shapiro^{1,2}

¹ *Department of Physics, University of Illinois at Urbana-Champaign,
Urbana, IL 61801-3080*

² *Department of Astronomy and NCSA, University of Illinois at Urbana-Champaign,
Urbana, IL 61801-3080*

ABSTRACT

Simulations in general relativity show that the outcome of collapse of a marginally unstable, uniformly rotating star spinning at the mass-shedding limit depends critically on the equation of state. For a very stiff equation of state, which is likely to characterize a neutron star, essentially all of the mass and angular momentum of the progenitor are swallowed by the Kerr black hole formed during the collapse, leaving nearly no residual gas to form a disk. For a soft equation of state with an adiabatic index $\Gamma - 4/3 \ll 1$, which characterizes a very massive or supermassive star supported predominantly by thermal radiation pressure, as much as 10% of the mass of the progenitor avoids capture and goes into a disk about the central hole. We present a semi-analytic calculation that corroborates these numerical findings and shows how the final outcome of such a collapse may be determined from simple physical considerations. In particular, we employ a simple energy variational principle with an approximate, post-Newtonian energy functional to determine the structure of a uniformly rotating, polytropic star at the onset of collapse as a function of polytropic index n , where $\Gamma = 1 + 1/n$. We then use this data to calculate the mass and spin of the final black hole and ambient disk. We show that the fraction of the total mass that remains in the disk falls off sharply as $3 - n$ (equivalently, $\Gamma - 4/3$) increases.

Subject headings: black hole physics – relativity – hydrodynamics – stars: rotation

1. Introduction

Determining the final state of a rotating star undergoing gravitational collapse is an important issue in relativistic astrophysics. Such a collapse is the principle route by which a rotating black hole forms in nature. Several different scenarios involving the collapse of rotating stars to black holes have been the focus of considerable attention recently. The collapse of massive stars in hypernovae explosions (“collapsars”) may be the origin of long-period gamma-ray bursts (MacFadyen & Woosley 1999; MacFadyen, Woosley & Heger 2001). The remnant of a binary neutron star, following inspiral and coalescence, is likely to be rapidly rotating and undergo collapse, either prompt or delayed, depending on its mass (Shibata & Uryu

2000, 2002; Baumgarte, Shapiro & Shibata 2000). Binary neutron star merger and collapse provides a plausible scenario for generating short-period gamma-ray bursts (Narayan, Paczynski & Piran 1992; Ruffert & Janka 1999) and a good candidate for the detection of gravitational waves by Advanced LIGO and other high-frequency, gravitational wave laser interferometers. The collapse of a rotating supermassive star may be a promising route for forming the seeds of supermassive black holes (see Shapiro 2003 for a review and references), which are likely to reside at the centers of many, and perhaps most, bulge galaxies (Richstone et al. 1998; Ho 1999), including the Milky Way (Genzel et al. 1997; Ghez et al. 2000; Schödel et al. 2002) and are believed to be the engines that power active galactic nuclei (AGNs) and quasars

(Rees 1998, 2001).

General relativity induces a radial instability in compact stars to catastrophic collapse. Rotation can support larger masses in stable equilibrium, but all stars become unstable to collapse when they are sufficiently compact. Uniformly rotating stars can have masses exceeding the maximum allowed mass of a nonrotating spherical star by about $\lesssim 20\%$. Cook, Shapiro & Teukolsky (1994a,b) have constructed numerical solutions of such “supramassive” stars, both for polytropes and for 14 realistic candidate nuclear equations of state. Differentially rotating stars can be “hypermassive”, with masses exceeding the maximum value for supramassive stars by factors of two or more (Baumgarte, Shapiro & Shibata 2000; Lyford, Baumgarte & Shapiro 2003). Viscosity (molecular or turbulent) and magnetic fields drive differentially rotating configurations to uniform rotation on secular timescales. [See, e.g., Shapiro 2000 and Cook, Shapiro & Stephens 2003 for recent Newtonian calculations of magnetic braking and viscous damping of differential rotation, and Liu & Shapiro 2004 for approximate, general relativistic calculations of these phenomena; see Duez et al. 2004 for detailed, general relativistic, numerical simulations of viscous damping of differential rotation.]

Here we focus on uniformly rotating stars and consider the collapse of supramassive stars. The first investigation of the gravitational collapse of supramassive stars was performed by Shibata, Baumgarte and Shapiro (2000), who employed a fully relativistic hydrodynamics code in three spatial dimensions plus time. They studied the collapse of a marginally unstable, relativistic polytrope with polytropic index $n = 1$ spinning at the mass-shedding limit. The mass-shedding limit is the maximal spin rate for a uniformly rotating star; here matter on the equator moves in a Keplerian (geodesic) orbit about the star, supported against gravity entirely by centrifugal forces. Stars with $n = 1$ have stiff equations of state, are not very centrally condensed and are fairly relativistic at the onset of collapse, with $R_e/M \approx 5.6$, where R_e is the equatorial (circumferential) radius and M is the total mass-energy. Such stars provide crude models of rapidly rotating, massive neutron stars. The outcome of collapse is a Kerr black hole containing all the rest-mass M_0 of the ini-

tial configuration, and essentially all of the total mass-energy M and angular momentum J of the initial configuration (apart from the small amount radiated away by gravitational waves). The reason that no matter remains outside the hole is that at the equator the specific angular momentum of the gas, which is strictly conserved during axisymmetric collapse, is smaller than j_{ISCO} , the specific angular momentum of a particle at the innermost stable circular orbit (ISCO) about the final hole. Hence all the interior matter in the star is captured by the hole. This situation is similar to the collapse of a nonrotating spherical star, which forms a Schwarzschild black hole without any ambient disk. By contrast, Shibata & Shapiro (2002) performed a fully relativistic hydrodynamics simulation in axisymmetry of the collapse of a marginally unstable $n = 3$ polytrope at the mass-shedding limit. Such a configuration models the likely endpoint state of an evolved, radiation-dominated, very massive or supermassive star at the onset of collapse (Baumgarte & Shapiro 1999). By contrast with an $n = 1$ polytrope, an $n = 3$ configuration has a soft equation of state, is very centrally condensed and is nearly Newtonian ($R_e/M \approx 620$) at the onset of collapse. A rotating black hole again forms during the collapse, but in this case the mass of the hole contains only about 90% of the total rest-mass of the system (with a spin parameter $J_h/M_h^2 \sim 0.75$). The remaining gas forms a rotating disk about the nascent hole. Here the angular momentum of the infalling matter in the outermost layers of the collapsing star exceeds j_{ISCO} , so the gas in the outer regions escapes capture and forms a disk. This result has been corroborated by a semi-analytic calculation by Shapiro & Shibata (2002), which we generalize below for arbitrary n .

Recently, Shibata (2003) performed systematic numerical simulations in axisymmetry to investigate the effects of the stiffness of the equation of state on the outcome of the collapse of marginally unstable, supramassive stars spinning at the mass-shedding limit. He studied collapsing relativistic polytropes with indices $2/3 \leq n \leq 2$, representing stiff and moderately stiff equations of state. He concluded that for these configurations the final state is a Kerr black hole and the disk mass, if it exists at all, is very small ($< 10^{-3}$ of the initial mass).

Simulations performed to date clearly show

that the outcome of the collapse of a maximally spinning, supramassive star depends critically on the equation of state. In this paper we employ a straightforward semi-analytic analysis to corroborate this conclusion and to show how the final outcome of these detailed simulations may be inferred from simple physical considerations. In particular, we employ an energy variational principle to determine the approximate structure of the marginally unstable, rotating star at the onset of collapse as a function of polytropic index n and use this data to estimate the mass and spin of the final black hole and ambient disk. We show that the mass of the disk depends sensitively on the difference $3 - n$. Our semi-analytic calculations are based on an approximate post-Newtonian energy functional valid for rotational energies that are much smaller than gravitational potential energies. They are most accurate for soft equations of state with n close to 3, since the parameters of the progenitor star are nearly Newtonian in this case and the effect of rotation in distorting the shape of the interior region containing most of the mass is minimal. Interestingly, stars with n close to 3 are the most difficult to simulate with a relativistic hydrodynamics code, since the large size of the progenitor star requires that any such code span an enormous dynamic range and integrate for a huge number of (Courant) timesteps in order to follow the collapse to completion and resolve the central black hole and disk reliably. In this sense, the two approaches – the semi-analytic analysis presented below and full numerical simulations – are complementary.

2. The Marginally Unstable, Supramassive Progenitor Star

In this Section we analyze the equilibrium and stability of a supramassive polytrope spinning at mass-shedding and identify the critical configuration at which radial instability sets in. Our treatment is a straightforward generalization to arbitrary polytropic index n of the semi-analytic analyses of Baumgarte & Shapiro (1999). We briefly review the predictions of the Roche approximation for the rotating envelope in Section 2.1. In Section 2.2 we present a post-Newtonian energy variational calculation which allows us to determine the critical configuration for each n and identify its two key parameters, R_p/M (where R_p is the

polar radius) and J/M^2 , needed to determine the mass and spin of the final black hole and disk. We calculate the mass and spin of the black hole and disk in Section 3. Henceforth we adopt geometrized units and set $G = c = 1$.

2.1. Review of the Newtonian Roche Model

Stars with soft equations of state are extremely centrally condensed: they have an extended, low density envelope, while the bulk of the mass is concentrated in the core. For an $n = 3$ Newtonian polytrope, for example, the ratio between central density to average density is $\rho_c/\bar{\rho} = 54.2$. The gravitational force in the envelope is therefore dominated by the massive core, and it is thus legitimate to neglect the self-gravity of the envelope. In the equation of hydrostatic equilibrium,

$$\frac{\nabla P}{\rho} = -\nabla(\Phi + \Phi_c), \quad (1)$$

this neglect amounts to approximating the Newtonian gravitational potential Φ by

$$\Phi = -\frac{M}{r} \quad (2)$$

In (1) we introduce the centrifugal potential Φ_c , which, for constant angular velocity Ω about the z -axis, can be written

$$\Phi_c = -\frac{1}{2}\Omega^2(x^2 + y^2) = -\frac{1}{2}\Omega^2 r^2 \sin^2 \theta. \quad (3)$$

Integrating eq. (1) yields the Bernoulli integral

$$h + \Phi + \Phi_c = H, \quad (4)$$

where H is a constant of integration and

$$h = \int \frac{dP}{\rho} = (n+1) \frac{P}{\rho} \quad (5)$$

is the enthalpy per unit mass. Here we have assumed a polytropic equation of state

$$P = K\rho^\Gamma, \quad K, \quad \Gamma = 1 + 1/n = \text{const}, \quad (6)$$

Evaluating eq. (4) at the pole yields

$$H = -\frac{M}{R_p}, \quad (7)$$

since $h = 0$ on the surface of the star and $\Phi_c = 0$ along the axis of rotation. In the following we assume that the polar radius R_p of a rotating star is always the same as in the nonrotating case. This assumption has been shown numerically to be very accurate (e.g., Papaloizou & Whelan 1973). The mass of the star is hardly changed from its value in spherical equilibrium, which to leading Newtonian order is given by the polytropic relation

$$M = 4\pi R_p^{(3-n)/(1-n)} \left[\frac{(n+1)K}{4\pi} \right]^{n/(n-1)} \times \xi_1^{(3-n)/(n-1)} \xi_1^2 |\theta'(\xi_1)|, \quad (8)$$

where the Lane-Emden functions for polytropes appearing above are tabulated in Chandrasekhar (1939). A rotating star reaches mass shedding when the equator orbits with the Kepler frequency. Using eqs. (3) and (4), it is easy to show that at this point the ratio between equatorial and polar radius is

$$\left(\frac{R_e}{R_p} \right)_{\text{shedd}} = \frac{3}{2}. \quad (9)$$

The corresponding maximum angular velocity is

$$\Omega_{\text{shedd}} = \left(\frac{2}{3} \right)^{3/2} \left(\frac{M}{R_p^3} \right)^{1/2} \quad (10)$$

(Zel'dovich & Novikov 1971; Shapiro & Teukolsky 1983).

Since the bulk of the matter is concentrated in the core and hardly affected by the rotation, the moment of inertia of the star barely changes with rotation and is well approximated by the nonrotating value

$$I = \frac{2}{5} \kappa_n M R_p^2, \quad (11)$$

where the nondimensional coefficient κ_n is tabulated for many different polytropes n in Lai, Rasio and Shapiro (1993) and for $n = 3$ and $n = 2.5$ in Table 1. The ratio between the kinetic and potential energy at mass-shedding then becomes

$$\begin{aligned} \left(\frac{T}{|W|} \right)_{\text{shedd}} &= \frac{(1/2)I\Omega_{\text{shedd}}^2}{(3/(5-n))M^2/R_p} \\ &= \left(\frac{8}{81} \right) (1 - n/5) \kappa_n. \end{aligned} \quad (12)$$

This result predicts that $T/|W|$ of a maximally rotating polytrope of index n is a universal constant, independent of mass, radius, or angular velocity.

Inserting eqs. (2), (3), and (5)–(10) into eq. (4) yields the density throughout the extended envelope,

$$\rho = \frac{\xi_1^{3-n} (\xi_1^2 |\theta'(\xi_1)|)^{n-1} M}{4\pi R_p^3} \left(\frac{R_p}{r} - 1 + \frac{4}{27} \frac{r^2}{R_p^2} \sin^2 \theta \right)^n. \quad (13)$$

The stellar surface is the boundary along which $\rho = 0$, and is thus defined by the curve $r(\theta)$ given by

$$\frac{4}{27} \frac{r^3}{R_p^3} \sin^2 \theta - \frac{r}{R_p} + 1 = 0. \quad (14)$$

The solution to this cubic equation is given by

$$\frac{r(\theta)}{R_p} = \frac{3 \sin(\theta/3)}{\sin \theta}. \quad (15)$$

2.2. Critical Configuration

To determine the equilibrium and stability of a rotating polytrope, we express its total energy as the sum of the (Newtonian) internal energy U , the potential energy W , the rotational energy T , a post-Newtonian correction E_{PN} and a post-post-Newtonian correction E_{PPN} . Writing the terms in that order yields the energy functional

$$\begin{aligned} E(\rho_c; M, J) &= k_1 K M \rho_c^{1/n} - k_2 M^{5/3} \rho_c^{1/3} \\ &\quad + k_3 j^2 M^{7/3} \rho_c^{2/3} - k_4 M^{7/3} \rho_c^{2/3} \\ &\quad - k_5 M^3 \rho_c, \end{aligned} \quad (16)$$

where ρ_c is the central density and where we have defined $j \equiv J/M^2$ and have neglected corrections due to deviations from sphericity. This neglect is justified, since these corrections scale with $T/|W|$, which according to (12) is always very small for centrally condensed configurations. Even though the value of the post-post-Newtonian correction E_{PPN} is very small, this term is crucial for determining the critical, marginally stable configuration for $n \equiv 3$, as emphasized by Zel'dovich and Novikov (1971) and Baumgarte & Shapiro (1999). The values of the nondimensional coefficients k_i are determined by quadratures over Lane-Emden functions. They are listed in Table 1 for $n = 3$ and $n = 2.5$; in our analysis below we evaluate them for arbitrary $2.5 \leq n \leq 3.0$ by linearly interpolating between these two values of n .

TABLE 1
VALUES OF THE POLYTROPIC STRUCTURE COEFFICIENTS

n	κ_n	k_1	k_2	k_3	k_4	k_5
3.0	0.18839 ^a	1.7558 ^a	0.63899 ^a	1.2041 ^a	0.91829 ^b	0.33121 ^c
2.5	0.27951 ^a	1.4295 ^a	0.67623 ^a	1.4202 ^a	0.86334 ^c	0.29752 ^c

Note that for any polytrope, $K^{n/2}$ has units of length. We can therefore introduce nondimensional coordinates by setting $K = 1$ (see Cook, Shapiro & Teukolsky 1992). We will denote values of nondimensional variables in these coordinates with a bar (for example \bar{M}). Values of these quantities for any other value of K can be recovered easily by rescaling with an appropriate power of $K^{n/2}$; for example $M = K^{n/2}\bar{M}$ and $\rho = K^{-n}\bar{\rho}$.

Taking the first derivative of eq. (16) with respect to the central density, holding M and J constant, yields the condition for hydrostatic equilibrium:

$$0 = \frac{\partial \bar{E}}{\partial x} = (3/n)k_1\bar{M}x^{(3/n-1)} - k_2\bar{M}^{5/3} + 2k_3j^2\bar{M}^{7/3}x - 2k_4\bar{M}^{7/3}x - 3k_5\bar{M}^3x^2, \quad (17)$$

where $x = \bar{\rho}_c^{1/3}$. For stable equilibrium, the second derivative of eq. (16) has to be positive. A root of the second derivative therefore marks the onset of radial instability:

$$0 = \frac{\partial^2 \bar{E}}{\partial x^2} = (3/n)(3/n-1)k_1\bar{M}x^{(3/n-2)} + 2k_3j^2\bar{M}^{7/3} - 2k_4\bar{M}^{7/3} - 6k_5\bar{M}^3x. \quad (18)$$

To find the critical configuration at mass-shedding, Eqs. (17) and (18) must be solved simultaneously for x and \bar{M} subject to the constraint

$$\frac{T}{|W|_{\text{shedd}}} = \frac{k_3j^2\bar{M}^{7/3}x^2}{k_2\bar{M}^{5/3}x} = \frac{k_3j^2\bar{M}^{2/3}x}{k_2}, \quad (19)$$

where the left hand side is given by eq. (12).

Key parameters characterizing the critical configurations are given in columns 2 – 4 of Table 2.

The first row for each n gives the solution found by solving eqs. (17) and (18) simultaneously, substituting eq. (19). The other rows for selected n give the results of a careful integration of the full Einstein equations of general relativity for the critical equilibrium configuration. The key global parameters needed to calculate the final black hole mass fraction and spin are the stellar compaction R_p/M and spin J/M^2 . The value of R_p/M determined by the simple variational method described above are seen to be most reliable for nearly Newtonian configurations with n close to 3. Nevertheless, as n decreases below 3 and the equation of state stiffens, the trend toward higher compaction at the critical point is clearly evident. The Newtonian Roche model for the outermost layers yields values for J/M^2 that are consistent with the exact model solutions, albeit these are somewhat low, even for n close to 3. The discrepancy arises from using eq. (11) for the moment of inertia, which neglects the increase in I arising from oblateness in the outer layers, and is strictly valid only for extreme central mass concentration¹.

3. Calculating the Black Hole Mass and Spin

In this section we generalize to arbitrary polytropic index n the iterative method of Shapiro & Shibata (2002) to calculate the mass and spin of the black hole and any disk that might form during the collapse of supramassive star. (They formulated the method for $n = 3$). Consider the implosion of matter from the envelope onto the central

¹A recalculation of the exact model by Shibata (2004) for $n = 3$ yields $J/M^2 = 0.91$, which removes much of the discrepancy.

TABLE 2
SUPRAMASSIVE STAR COLLAPSE VS. POLYTROPIC INDEX n

n	Critical Supramassive Star			Final Black Hole and Disk		
	\bar{M}	R_p/M	J/M^2	M_h/M	J_h/M_h^2	M_d/M
3.00	4.56	456	0.876	0.89	0.60	0.11
	4.57 ^a	427 ^a	0.97 ^a	0.87	0.71	0.13
	4.57 ^a	427 ^a	0.97 ^a	0.9 ^c	0.75 ^c	0.1 ^c
2.95	3.83	196	0.602	0.97	0.52	0.029
2.90	3.30	119	0.491	0.99	0.45	0.011
	3.30 ^b	122 ^b	0.567 ^b	0.99	0.53	0.014
2.80	2.54	60.9	0.382	1.00	0.37	2.5×10^{-3}
2.70	2.02	37.7	0.325	1.00	0.32	5.3×10^{-4}
2.60	1.65	25.5	0.287	1.00	0.29	9.7×10^{-5}
2.50	1.38	18.2	0.259	1.00	0.26	1.2×10^{-5}
	1.29 ^b	28.9 ^b	0.389 ^b	1.00	0.39	2.7×10^{-4}

^aBaumgarte & Shapiro (1999), Table 2

^bCook, Shapiro & Teukolsky (1994a), Table 2, converting R_e to R_p using $R_p/R_e \approx 2/3$.

^cRelativistic hydrodynamics simulation by Shibata & Shapiro (2002)

black hole formed from the collapse of the centrally condensed interior region. If the specific angular momentum of the imploding envelope matter is below j_{ISCO} , the specific angular momentum of a particle at the innermost stable circular orbit (ISCO) about the hole, the matter will be captured. If the angular momentum of the infalling matter exceeds j_{ISCO} , the matter will escape capture and continue to orbit outside the hole, forming a disk. This capture criterion is well-supported by the numerical simulations of rotating collapse by Shibata & Shapiro (2002) for $n = 3$ stars and by Duez et al. (2004) for $n = 1$ stars. In both cases the capture of fluid in orbits with $j > j_{\text{ISCO}}$ was demonstrated to be negligible. This criterion suggests a simple iterative scheme for calculating the final mass and spin of the hole and disk from the initial stellar density and angular momentum profile. First, guess the mass and spin of the hole, M_h and J_h . For our initial guess, we shall take a black hole that has consumed all the mass and angular momentum of the star, so that $M_h/M = 1$ and $J_h/M_h^2 = (J/M^2)_{\text{crit}}$. Next, use the initial stellar density and angular momentum profiles to “cor-

rect” this guess by calculating the escaping mass and angular momentum of the outermost envelope with specific angular momentum exceeding j_{ISCO} . We note that the value j_{ISCO} depends on M_h and J_h . We then “correct” the black hole mass and spin by deducting the values of the escaping mass and angular momentum of the envelope material from the guessed values of M_h and J_h . We recompute j_{ISCO} for the “corrected” black hole mass and spin, and repeat the calculation of the escaping envelope mass and angular momentum until convergence is achieved. The calculation described exploits the theorem that for an axisymmetric dynamical system, the specific angular momentum spectrum, i.e., the integrated baryon rest-mass of all fluid elements with specific angular momentum j less than a given value (e.g., j_{ISCO}) is strictly conserved in the absence of viscosity (Stark & Piran 1987). Any viscosity, if present, is expected to be unimportant on dynamical timescales, as required by the theorem.

For a Kerr black hole of mass M_h and spin parameter $a = J_h/M_h$, the value of j_{ISCO} is given

by

$$j_{\text{ISCO}} = \frac{\sqrt{M_h r_{\text{ms}}}(r_{\text{ms}}^2 - 2a\sqrt{M_h r_{\text{ms}}} + a^2)}{r_{\text{ms}}(r_{\text{ms}}^2 - 3M_h r_{\text{ms}} + 2a\sqrt{M_h r_{\text{ms}}})^{1/2}}, \quad (20)$$

where r_{ms} is the ISCO given by

$$r_{\text{ms}} = M_h \{3 + Z_2 - [(3 - Z_1)(3 + Z_1 + 2Z_2)]^{1/2}\}, \quad (21)$$

where

$$Z_1 \equiv 1 + \left(1 - \frac{a^2}{M_h^2}\right)^{1/3} \left[\left(1 + \frac{a}{M_h}\right)^{1/3} + \left(1 - \frac{a}{M_h}\right)^{1/3} \right], \quad (22)$$

and

$$Z_2 \equiv \left(3 \frac{a^2}{M_h^2} + Z_1^2\right)^{1/2} \quad (23)$$

(see, e.g., Shapiro & Teukolsky 1983). Clearly, the infalling gas corotates with the black hole.

The mass of the escaping matter in the envelope with $j > j_{\text{ISCO}}$ is given by

$$\Delta M = \iint 2\pi\varpi d\varpi\rho, \quad (24)$$

where the density is given by eq. (13) and the quadrature is performed over all cylindrical shells in the star with cylindrical radii $\varpi > \varpi_{\text{ISCO}} = (j_{\text{ISCO}}/\Omega)^{1/2}$. Here we set $\Omega = \Omega_{\text{shedd}}$ given by eq. (10). (The quantity computed in eq. (24) is actually the escaping rest-mass, but when the envelope is nearly Newtonian, as we assume here, we can neglect the small difference between rest-mass and total mass-energy.) Defining $\bar{\varpi} = \varpi/R_p$ and $\bar{z} = z/R_p$ gives the nondimensional integral

$$\Delta M/M = \xi_1^{(3-n)} (\xi_1^2 |\theta'(\xi_1)|)^{(n-1)} \times \iint \bar{\varpi} d\bar{\varpi} d\bar{z} \left[\frac{1}{(\bar{\varpi}^2 + \bar{z}^2)^{1/2}} - 1 + \frac{4}{27} \bar{\varpi}^2 \right]^n. \quad (25)$$

Similarly, the angular momentum carried off by the escaping matter in the envelope is given by

$$\Delta J = \iint 2\pi\varpi d\varpi\rho\Omega\varpi^2 \quad (26)$$

or

$$\Delta J/M^2 = \xi_1^{(3-n)} (\xi_1^2 |\theta'(\xi_1)|)^{(n-1)} \left(\frac{2}{3}\right)^{3/2} \left(\frac{R_p}{M}\right)^{1/2} \times \iint \bar{\varpi}^3 d\bar{\varpi} d\bar{z} \left[\frac{1}{(\bar{\varpi}^2 + \bar{z}^2)^{1/2}} - 1 + \frac{4}{27} \bar{\varpi}^2 \right]^n, \quad (27)$$

where R_p/M is given in Table 2 and where once again the integral is performed over all cylindrical shells in the star with $\varpi > \varpi_{\text{ISCO}} = (j_{\text{ISCO}}/\Omega)^{1/2}$. Eqns. (25) and (27) agree with Shapiro & Shibata (2002), eqns. (22) and (24), for $n = 3$.

The mass and angular momentum of the black hole can then be determined from eqs. (25) and (27) according to

$$M_h/M = 1 - \Delta M/M \quad (28)$$

and

$$J_h/M_h^2 = \frac{(J/M^2 - \Delta J/M^2)}{(1 - \Delta M/M)^2}. \quad (29)$$

Once the iteration of eqs. (20) – (23) with eqs. (25), (28) and (29) converges, the mass of the ambient disk can be found from

$$M_{\text{disk}}/M = \Delta M/M. \quad (30)$$

Typically, convergence to better than 1% is achieved after only four iterations.

The calculated parameters for the final black hole and disk are given in the last three columns of Table 2 for different values of n . The values for $n = 3$ are the most reliable, since the calculation of the density and angular momentum distributions in the outermost layers by means of a Newtonian Roche model is most accurate for such a soft equation of state. For $n = 3$ we are able to compare the semi-analytic calculations with the numerical collapse simulation of Shibata & Shapiro (2002). Allowing for numerical error inherent in the simulation (\lesssim few percent), the agreement is quite good for the final masses of the black hole and disk, and reasonable, but less accurate, for the final black hole spin. The numerical simulation (third row in Table 2) used an initial model obtained by a numerical integration of the full general relativistic, equilibrium equations for the critical configuration at the onset of collapse. When the parameters for this model are also used in the analytic derivation of the final black hole and disk (second row in Table 2) in place of the values determined by the variational principle (first row in Table 2), the agreement with the spin is much improved.

The dependence of the black hole spin and disk mass on the polytropic index is summarized in Figures 1 and 2. The spin parameter increases moderately with increasing n and increasing central

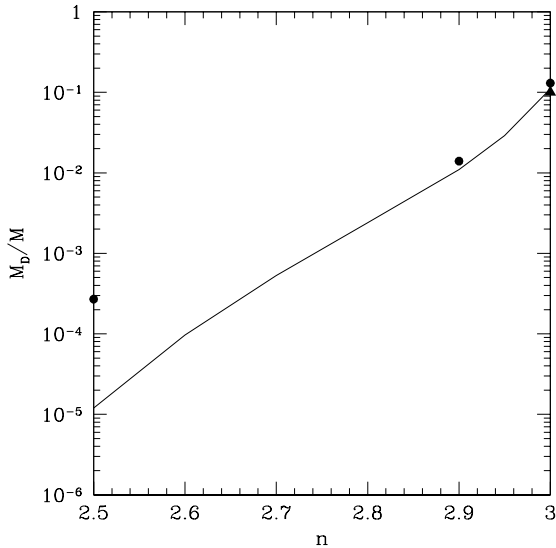


Fig. 1.— Mass-fraction of the disk formed following collapse of a marginally unstable, supra-massive polytrope at the mass-shedding limit versus polytropic index. The solid line uses critical star parameters given by the variational treatment. The solid dots use critical parameters determined from numerical models of marginally unstable, relativistic equilibrium stars at the mass-shedding limit (see Table 2). The solid triangle shows the value determined by a numerical simulation by Shibata & Shapiro (2002).

concentration in the critical star. The disk mass is far more sensitive to the equation of state and increases very rapidly with increasing n . There is hardly any mass in the disk unless n is very close to 3, a result which is consistent with the dynamical simulations of Shibata, Baumgarte & Shapiro (2000) and Shibata (2003) covering the range $2/3 \leq n \leq 2$.

4. Application: Very Massive Star Collapse

A very massive, uniformly rotating star ($M/M_\odot \gg 100$) is characterized by the following properties:

1. It is dominated by thermal radiation pressure;
2. It is fully convective;

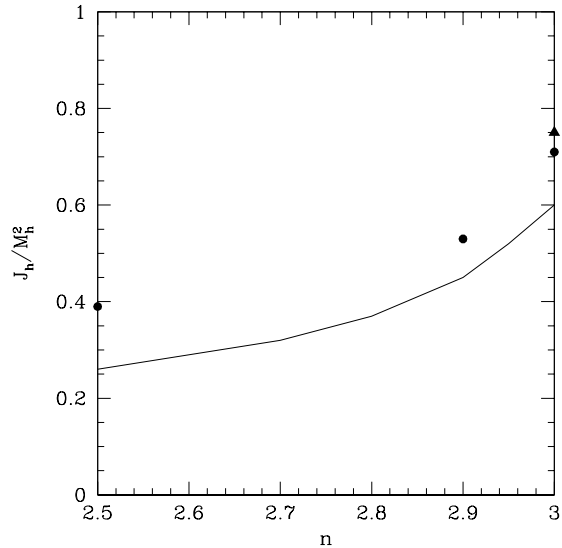


Fig. 2.— Spin-parameter of the black hole formed following collapse of a marginally unstable, supra-massive polytrope at the mass-shedding limit versus polytropic index. The curves and points are labelled as in Fig 1.

3. It is governed by nearly Newtonian gravitation;
4. It is described by the Roche model in the outer envelope.

Such stars behave as polytropes with adiabatic index $\Gamma = 1 + 1/n$ given by

$$\Gamma \approx 4/3 + \beta/6 + \mathcal{O}(\beta^2), \quad \beta \equiv \frac{P_g}{P_r}, \quad (31)$$

where $P_r = \frac{1}{3}aT^4$ is the radiation pressure and $P_g = nkT/\mu$ is the gas pressure (see, e.g., Shapiro & Teukolsky 1983, Chapter 17). The ratio $\beta \ll 1$ is related to the radiation entropy per baryon s_r (\approx constant throughout the star) according to $\beta = (4/\mu)/(s_r/k)$, where μ is the mean molecular weight, while the mass is related to the entropy according to

$$s_r/k \approx 0.942(M/M_\odot). \quad (32)$$

Combining the above equations and evaluating $\mu \approx 2/(1 + 3X + 0.5Y)$ for a zero-metallicity, primordial composition ($X = 0.75$ and $Y = 0.25$; Cyburt, Fields and Olive 2003) likely to characterize

massive Population III objects, yields, to lowest order,

$$M/M_{\odot} \approx \frac{116}{(3-n)^2}. \quad (33)$$

Baumgarte & Shapiro (1999) have shown that, following cooling and contraction, such a massive star will likely settle into rigid rotation and evolve to the mass-shedding limit, assuming the viscous or magnetic braking timescale for angular momentum transfer is shorter than the evolution timescale in such an object (Bisnovatyi-Kogan et al. 1967; Zel'dovich & Novikov 1971; Shapiro 2000; but see New & Shapiro 2001 for an alternative scenario). Moreover, Newtonian simulations suggest that zero-metallicity rotating stars with $M/M_{\odot} \gtrsim 260$ do not encounter the pair-production instability, so they collapse to black holes without exploding (Fryer, Woosley & Heger 2001). The relation derived above between the mass M and polytropic index n for very massive stars then permits us to apply the results of the previous section to determine the final fate of these objects after they reach the onset of radial instability and collapse. For example, if the star has a mass $M/M_{\odot} \gtrsim 10^4$, then $3-n \lesssim 0.1$. So according to Table 2 and Figs 1 and 2, the spin of the resulting hole will be moderate, $J_h/M_h^2 \gtrsim 0.5$, and the mass of the disk leftover from the collapse will be nonnegligible, $M_D/M \gtrsim 10^{-2}$. The relativistic simulations of Shibata & Shapiro 2002 for pure $n=3$ polytropes serve to confirm these predictions in the limiting regime $3-n \ll 1$.

5. Summary and Conclusions

We have employed a simple analysis to determine the effect of the stiffness of the equation of state on the fate of the collapse of a marginally unstable, relativistic polytrope spinning uniformly at the mass-shedding limit. We have used a variational principle and an approximate, post-Newtonian energy functional to determine the key parameters defining the structure of the critical progenitor star. We compared these parameters with the results of detailed numerical model calculations of stationary configurations for select cases. We then employed a Roche model to obtain analytic expressions for the density and angular momentum profiles in the envelope of the marginally stable star. We substituted these pro-

files into quadratures that determine the fractions of the stellar mass and angular momentum which escape capture by the central black hole assumed to form during the collapse. The fraction of the progenitor mass and spin which go into the hole versus the ambient disk is then iterated until convergence is achieved.

We find that for the stars treated here, the mass fraction in the disk is about 10% for an $n=3$ polytrope and decreases rapidly as n decreases and the equation of state stiffens. The results are in agreement with the numerical simulations in $3+1$ by Shibata, Baumgarte & Shapiro (2000) for $n=1$ and simulations by Shibata (2003) in axisymmetry for $2/3 \leq n \leq 2$, which show that the mass fraction in a disk, if present at all, is less than 0.1% of the total mass. For the special case of $n=3$, the results are also in agreement with the simulation performed by Shibata & Shapiro (2002) in axisymmetry, as has been discussed previously by Shapiro and Shibata (2002). The spin parameter of the black hole is less sensitive to the stiffness of the equation of state, decreasing from $J_h/M_h^2 \approx 0.75$ for $n=3$ to $J_h/M_h^2 \approx 0.39$ for $n=2.5$.

The approach outlined here is more reliable for soft equations of state. In this limit the marginally unstable configuration is nearly Newtonian and the post-Newtonian energy functional describing the bulk of the mass, the Newtonian Roche model describing the envelope and the quadrature determining the escaping mass-energy fraction (assumed to equal the escaping rest-mass fraction) all become better approximations. Interestingly, this is precisely the limit where fully relativistic numerical simulations become more taxing, due to the large dynamic range and very long time integrations required for a hydrodynamic calculation.

While the semi-analytic approach presented here to predict the final black hole and disk masses and spins was applied to treat the collapse of stars with *uniform* rotation, the method can be used equally well to treat the collapse of unstable stars with *differential* rotation. Recently, Duez et al. (2004) performed fully relativistic numerical simulations of hypermassive stars with appreciable differential rotation. Hypermassive stars may form from the merger of binary neutron stars or from rotating core collapse in supernovae (Baumgarte, Shapiro & Shibata 2000). Magnetic braking or viscous damping of differential rotation in such

stars can drive them unstable to collapse on secular timescales. Duez et al. (2004) performed simulations to demonstrate this effect in the case of viscosity and showed that the final black hole and disk parameters are in agreement with the values predicted by the method outlined in Section 3. In particular, they showed that for rapid differential rotation characteristic of hypermassive stars, the disk mass fraction is typically large (10% – 20% of the total initial mass) for stiff equations of state with $n = 1$. We therefore conclude that, in general, the parameters of the final black hole and the disk formed during the collapse of an unstable star depend both on the equation of state and on the degree of differential rotation.

It is a pleasure to thank T. W. Baumgarte, C. F. Gammie, and M. Shibata, for valuable discussions. This work was supported in part by NSF Grants PHY-0090310 and PHY-0205155 and NASA Grant NAG5-10781 at the University of Illinois at Urbana-Champaign.

REFERENCES

- Baumgarte, T. W. & Shapiro, S. L., 1999, *ApJ*, 526, 941.
- Baumgarte, T. W., Shapiro, S. L. & Shibata, M. 2000, *ApJ*, 528, L29.
- Bisnovatyi-Kogan, G. S., Zel'dovich, Ya. B., & Novikov, I. D., 1967, *Soviet Astron.*, 11, 419.
- Chandrasekhar, S., 1939, *An Introduction to the Study of Stellar Structure*, (Dover, New York).
- Cook, G. B., Shapiro, S. L. & Teukolsky, S. A., 1992, *ApJ*, 398, 203.
- Cook, G. B., Shapiro, S. L. & Teukolsky, S. A., 1994a, *ApJ*, 422, 227.
- Cook, G. B., Shapiro, S. L. & Teukolsky, S. A., 1994b, *ApJ*, 424, 823.
- Cook, J. N., Shapiro, S. L. & Stephens, B. C. 2003, *ApJ*, in press (astro-ph/0310304).
- Cybur, R. H., Fields, B. D. & Olive, K. A., 2003, *Phys. Lett. B* 567, 227.
- Duez, M. D., Liu, Y. T., Shapiro, S. L. & Stephens, B. C. 2004, *PRD* in press, (astro-ph/0402502).
- Fryer, C. L., Woosley, S. E. & Heger, A., 2001, *ApJ*, 550, 372.
- Genzel, R., Eckart, A., Ott, T. & Eisenhauer, F. 1997, *MNRAS*, 291, 219
- Ghez, A. M., Morris, M., Becklin, E. E., Tanner, A. & Kremenek, T. 2000, *Nature*, 407, 349
- Ho, L. C. 1999, in *Observational Evidence for Black Holes in the Universe*, ed. S. K. Chakrabarti (Kluwer: Dordrecht), 157
- Lai, D., Rasio, F. A. & Shapiro, S. L. 1993, *ApJ Supp.*, 88, 205.
- Liu, Y. T. & Shapiro, S. L., 2004, *PRD*, in press (astro-ph/0312038).
- Lyford, N. D., Baumgarte, T. W. & Shapiro, S. L. 2003, *ApJ*, 583, 410.
- MacFadyen, A. I. & Woosley, S. E., 1999, *ApJ*, 524, 262.
- MacFadyen, A. I., Woosley, S. E. & Heger, A., 2001, *ApJ*, 550, 410.
- New, K. C. B. & Shapiro, S. L., 2001, *ApJ*, 548, 439.
- Narayan, R. & Yi, I., 1994, *ApJ*, 428, L13.
- Narayan, R., Paczynski, B. & Piran, T., 1992, *ApJ*, 395, L83.
- Papaloizou, J. C. B., & Whelan, F. A. J., 1973, *MNRAS*, 164, 1.
- Rees, M. J., 1998, in *Black holes and relativistic stars*, ed. R. M. Wald (Chicago University Press, Chicago), 79.
- Rees, M. J., 2001, in *Black holes in Binaries and Galactic Nuclei*, ed. L. Kaper, E. P. J. van den Heuvel, & P. A. Woudt (Springer-Verlag: New York), 351.
- Richstone, D., et al. 1998, *Science*, 395, A14.
- Ruffert, M. & Janka, H.-Th., 1999, *A&A*, 344, 573.
- Shapiro, S. L., 2000, *ApJ*, 544, 397.
- Shapiro, S. L., 2003, in *The Astrophysics of Gravitational Wave Sources*, ed. J. M. Centrella (AIP, Melville, New York), 50.

- Shapiro, S. L. & Shibata, M., 2002, ApJ, 577, 904.
- Shapiro, S. L. & Teukolsky, S. A., 1983, Black Holes, White Dwarfs, and Neutron Stars (Wiley interscience, New York).
- Schödel, R., et al. 2002, Nature, 419, 694
- Shibata, M., 2000, Prog. Theor. Phys, 104, 325.
- Shibata, M., 2003, ApJ, 595, 992.
- Shibata, M., 2004, astro-ph/0403172.
- Shibata, M., Baumgarte, T. W. & Shapiro, S. L., 2000, Phys. Rev. D 61, 044012.
- Shibata, M. & Shapiro, S. L., 2002, ApJ, 572, L39.
- Shibata, M. & Uryu, K. 2000, PRD, 61, 064001.
- Shibata, M. & Uryu, K. 2002, Prog. Theor.Phys., 107, 265.
- Stark, R. F. & Piran, T., 1987, Comp. Phys. Rep., 5, 221.
- Zel'dovich, Ya. B. & Novikov, I. D., 1971, Relativistic Astrophysics Vol. 1 (University of Chicago Press, Chicago).